

# The High-Temperature Phase of Landau-Gauge Yang-Mills Theory

Axel Maas<sup>1</sup>, Jochen Wambach<sup>1,2</sup>, and Reinhard Alkofer<sup>3</sup>

<sup>1</sup> Gesellschaft für Schwerionenforschung mbH, Planckstr. 1, D-64291 Darmstadt, Germany

<sup>2</sup> Institute for Nuclear Physics, Darmstadt University of Technology, Schloßgartenstraße 9, D-64289 Darmstadt, Germany

<sup>3</sup> Institute of Physics, University of Graz, Universitätsplatz 5, A-8010 Graz, Austria

Received: date / Revised version: date

**Abstract.** The properties of the high-temperature phase of Yang-Mills theory in Landau gauge are investigated by extending an earlier study on the infinite-temperature limit to finite temperatures. To this end the Dyson-Schwinger equations for the propagators of the gluon and the Faddeev-Popov ghost are solved analytically in the infrared and numerically at non-vanishing momenta. Gluons, polarized transversely with respect to the heat bath are found to comply with the Gribov-Zwanziger and the Kugo-Ojima scenario, while longitudinally polarized gluons are screened. Therefore the high-temperature phase is strongly interacting. It is furthermore conjectured that Yang-Mills theory undergoes a first-order phase transition. Indications are found that at high temperatures the thermodynamic properties are nearly those of an ideal gas, although long-range interactions prevail.

**PACS.** 11.10.Wx Finite-temperature field theory – 11.15.-q Gauge field theories – 12.38.-t Quantum chromodynamics – 12.38.Aw General properties of QCD – 12.38.Lg Other nonperturbative calculations – 12.38.Mh Quark-gluon plasma – 14.70.Dj Gluons

## 1 Introduction

The high-temperature phase of QCD and even of pure Yang-Mills theory remains a largely unsolved problem. The equation of state, as found in lattice calculations, exhibits an almost trivial Stephan-Boltzmann behavior of the ideal gas. However, perturbation theory fails (for a recent review see e.g. [1]). In addition, in the limit of infinite temperature, at least part of the gluon spectrum shows confinement [2] in accordance with the scenarios of Kugo and Ojima [3] and of Gribov and Zwanziger [4, 5]. This clearly demonstrates that nonperturbative quantum effects persist in that limit.

The objective here is to understand the properties of the gluons and Faddeev-Popov ghosts, in particular in the infrared, in the high-temperature phase. This work is therefore an extension of studies at infinite temperature [2] and complements studies at temperatures below the phase transition [6].

To accomplish this task, the Dyson-Schwinger equations (DSEs) [7] for the propagators of the gluon and the Faddeev-Popov ghost are investigated. A clear separation of soft and hard degrees of freedom is found. Indications will be discussed that this separation of scales is the reason why a microscopically highly non-trivial and especially nonperturbative theory can exhibit quite simple macroscopic properties as is the case for the equation of state.

The paper is organized as follows. In section 2 Yang-Mills theory and signals of confinement are briefly reviewed. The Dyson-Schwinger equations are introduced in section 3. An analytical treatment of the infrared sector is given in section 4. The consequences of the necessary truncations and renormalization will be discussed in section 5. Numerical solutions beyond the infrared will be presented in section 6. This includes comments on the thermodynamic potential and Schwinger functions. A discussion of the results and the phase structure are finally given in section 7. A summary and concluding remarks close the paper in section 8. Some technical issues are deferred to two appendices.

## 2 Aspects of Yang-Mills theory

The following investigations are restricted to pure Yang-Mills theory as substantial evidence exists that the non-perturbative features of QCD are generated in the gauge sector. Hence, the theory studied here is an equilibrium Yang-Mills theory governed by the Euclidean Lagrangian<sup>1</sup> [8, 9]

$$\mathcal{L} = \frac{1}{4} F_{\mu\nu}^a F_{\mu\nu}^a + \bar{c}^a \partial_\mu D_\mu^{ab} c^b$$

<sup>1</sup> The hermiticity assignment for the ghosts is different from the conventional, although valid for Landau gauge [8].

$$F_{\mu\nu}^a = \partial_\mu A_\nu^a - \partial_\nu A_\mu^a - g f^{abc} A_\mu^b A_\nu^c,$$

$$D_\mu^{ab} = \delta^{ab} \partial_\mu + g f^{abc} A_\mu^c.$$

Here  $F_{\mu\nu}^a$  denotes the field strength tensor,  $D_\mu^{ab}$  the covariant derivative,  $g$  the gauge coupling and  $f^{abc}$  the structure constant of the gauge group, which is SU(3) unless otherwise noted.  $A_\mu^a$  denotes the gluon field, and  $\bar{c}^a$  and  $c^a$  are the Faddeev-Popov ghost fields describing part of the quantum fluctuations of the gluon field. We choose the Landau gauge, which for technical reasons is best suited for the purpose at hand [8].

The main focus of the present work is the fate of confinement at temperatures above the phase transition. It is therefore necessary to be able to extract information about confinement. Part of this information is encoded in the pertinent 2-point functions. The corresponding signals will be only listed here. For a brief introduction to confinement in covariant gauges see ref. [10].

A sufficient criterion for the presence of confinement is based on the fact that no Källén-Lehmann representation of a particle exists if its spectral function is not positive semi-definite. It is then not part of the physical spectrum and thus confined, c.f. [11]. This is the case if the corresponding propagator  $D$  vanishes at zero momentum,

$$\lim_{p^2 \rightarrow 0} D(p^2) = 0. \quad (1)$$

This is essentially the behavior expected for the propagator of a confined gluon.

The two remaining criteria stem from possible confinement mechanisms. The Kugo-Ojima scenario [3] puts forward the idea that all colored objects are BRST charged and thus unphysical. One precondition for this mechanism is an unbroken global color charge. In the Landau gauge this condition can be cast into [12]

$$\lim_{p^2 \rightarrow 0} p^2 D_G(p^2) \rightarrow \infty, \quad (2)$$

where  $D_G$  is the propagator of the Faddeev-Popov ghosts. This scenario necessarily also implies the condition (1) for the gluon propagator.

In the Gribov-Zwanziger scenario [5], entropy arguments are employed to show the dominance of field configurations close or on the Gribov horizon in field configuration space. This scenario predicts again condition (2). For an infrared constant ghost-gluon vertex, which is supported by lattice calculations [13] and semi-perturbative calculations [14], condition (1) follows as well for the gluon propagator [5].

Also intuitively it is clear that a strongly divergent ghost propagator at zero momentum can mediate confinement. Such an infrared divergence relates to long-ranged spatial correlations. These are stronger than the ones induced by a Coulomb force since the divergence in momentum space is stronger than that of a massless particle. An infrared vanishing gluon propagator is also intuitively linked to confinement, as  $p^2 = 0$  puts a non-interacting gluon on-shell. Thus the gluon does not propagate and is confined.

### 3 Dyson-Schwinger equations

The DSEs [7,8] form an infinite tower of coupled non-linear integral equations for the Green's functions of a given theory. Therefore, in general only a truncated set can be solved in practical calculations. In the following we aim at a closed set of equations for the pertinent 2-point functions. In Landau gauge and at finite temperature these are the ghost propagator

$$D_G(p) = \frac{-G(p_0^2, \mathbf{p}^2)}{p^2} \quad (3)$$

and the gluon propagator [9]

$$D_{\mu\nu}(p) = P_{T\mu\nu}(p) \frac{Z(p_0^2, \mathbf{p}^2)}{p^2} + P_{L\mu\nu}(p) \frac{H(p_0^2, \mathbf{p}^2)}{p^2}. \quad (4)$$

where  $P_T$  and  $P_L$  are projectors transverse and longitudinal w.r.t. the heat-bath. Eqs. (3) and (4) define the dimensionless dressing functions  $G(p_0^2, \mathbf{p}^2)$ ,  $Z(p_0^2, \mathbf{p}^2)$ , and  $H(p_0^2, \mathbf{p}^2)$ .

The derivation of the Dyson-Schwinger equations is a straightforward, but tedious task. As in the previous investigations [2,6], we follow here ref. [15] and keep only the equations for the propagators. Furthermore we neglect one-particle-irreducible two-loop diagrams and assume a perturbative color structure. Furthermore, the ghost-gluon vertex is taken to be bare, in accordance with recent investigations [13,14]. The construction of the various three-gluon vertices will be discussed in section 5.

The equations are obtained from the vacuum equations (see e.g. ref. [8]) by application of the Matsubara formalism [9]. To obtain scalar equations for the (infinite) set of Matsubara frequencies of the dressing functions  $Z$  and  $H$  of the gluon propagator (4), the gluon equation is contracted with the generalized projectors  $P_{T\mu\nu}^\zeta$  and  $P_{L\mu\nu}^\xi$ , respectively, defined by<sup>2</sup>

$$P_{T\mu\nu}^\zeta = \zeta P_{T\mu\nu} + (\zeta - 1) (\delta_{\mu\nu} - \delta_{\mu 0} \delta_{0\nu}), \quad (5)$$

$$P_{L\mu\nu}^\xi = \xi P_{L\mu\nu} + (\xi - 1) \left( \delta_{\mu 0} \frac{p_0 p_\nu}{p^2} + \delta_{0\nu} \frac{p_\mu p_0}{p^2} \right). \quad (6)$$

The choice of the projectors was made so as to obtain a well-defined 3-dimensional limit. The parameters  $\zeta$  and  $\xi$  allow to vary the projection continuously in order to investigate the amount of gauge symmetry violations. The dependence on  $\xi$  vanishes in the infinite-temperature limit [2].

Employing the projectors (5) and (6) yields the finite temperature DSEs as

$$\frac{1}{G(p)} = \tilde{Z}_3$$

<sup>2</sup> These are chosen differently from the ones in ref. [2] to avoid an inconvenient kinematical singularity. In the limit of infinite temperature, the resulting equations for the soft modes are the same.

$$+ \frac{g^2 T C_A}{(2\pi)^2} \sum_{n=-\infty}^{\infty} \int d\theta d|\mathbf{q}| \left( A_T(p, q) G(q) Z(p-q) \right. \\ \left. + A_L(p, q) G(q) H(p-q) \right) \quad (7)$$

$$\frac{\xi}{H(p)} = \xi Z_{3L} + T^{HG} + T^{HH} \\ + \frac{g^2 T C_A}{(2\pi)^2} \sum_{n=-\infty}^{\infty} \int d\theta d|\mathbf{q}| \left( P(p, q) G(q) G(p+q) \right. \\ \left. + N_L(p, q) Z(q) Z(p+q) + N_1(p, q) H(q) Z(p+q) \right. \\ \left. + N_2(p, q) H(p+q) Z(q) + N_T(p, q) H(q) H(p+q) \right) \quad (8)$$

$$\frac{1}{Z(p)} = Z_{3T} + T^{GH} + T^{GG} \\ + \frac{g^2 T C_A}{(2\pi)^2} \sum_{n=-\infty}^{\infty} \int d\theta d|\mathbf{q}| \left( R(p, q) G(q) G(p+q) \right. \\ \left. + M_L(p, q) H(q) H(p+q) + M_1(p, q) H(q) Z(p+q) \right. \\ \left. + M_2(p, q) H(p+q) Z(q) + M_T(p, q) Z(q) Z(p+q) \right) \\ + \frac{p_0^2(\zeta-1)}{2p^2} \left( Z_{3L} - \frac{1}{H(p)} \right). \quad (9)$$

Here  $C_A = f^{abc} f_{abc} = N_c$  is the adjoint Casimir of the gauge group. The summation runs over all Matsubara frequencies  $q_0 = 2\pi T n$ . This (truncated) set of DSEs is graphically displayed in Fig. 1.

The  $\zeta$  and  $\xi$  dependence of the DSEs is acquired by using (5) and (6). At  $\zeta = \xi = 1$  the original form of the equations is recovered. For  $p_0 = 0$ , equation (8) is only superficially dependent on  $\xi$ . As all integral kernels are in this case proportional to  $\xi$ , the dependence can be divided out for  $\xi \neq 0$ . Then, only the implicit dependence through interactions with the hard modes remains. The latter effect vanishes in the infinite-temperature limit and (8) becomes the equation for the Higgs field of [2], independent of  $\xi$ .

The finite-temperature theory is renormalizable. Thus, explicit wave-function renormalization constants  $\tilde{Z}_3$ ,  $Z_{3L}$ , and  $Z_{3T}$  have been introduced and will be discussed in section 5. Concerning the vertex renormalization,  $\tilde{Z}_1 = 1$  has been employed for the ghost-gluon vertex [16]. The three-gluon vertex renormalization constant  $Z_1$  cannot be calculated in the present truncation, but it is finite and set to 1 [17, 18]. The kernels  $A_T$ ,  $A_L$ ,  $R$ ,  $M_T$ ,  $M_1$ ,  $M_2$ ,  $M_L$ ,  $P$ ,  $N_T$ ,  $N_1$ ,  $N_2$ , and  $N_L$  contain trivial factor such as the integral measure. The integral kernels are quite lengthy, and will not be displayed here. They can be found in ref. [19].

The tadpoles  $T^{ij}$  are used to cancel spurious divergences in much the same way as in ref. [2], see section 5. However, also in the soft equations, they can possess finite parts at finite temperature. In case of the longitudinal equation, these can be absorbed into the mass renormalization discussed below. In the transverse equation, these are at  $\zeta = 3$  completely contained in the loop terms, and

their continuation away from  $\zeta = 3$  is thus arbitrary. Also these contributions scale at best only as  $1/p^2$  in the infrared and thus turn out to be irrelevant. Therefore, they are dropped, especially as no simple prescription as the one given later in Eq. (23) can remove the related spurious divergences

Close inspection of the equations reveals further that the dressing functions can only depend on  $|p_0|$  and  $|\mathbf{p}|$ . The corresponding symmetry, under  $p_0 \rightarrow -p_0$ , is used to reduce the number of equations significantly.

Eqs. (7-9) depend on the coupling constant  $g$  as the only parameter. In turn,  $g$  depends on the renormalization scale  $\mu$ , which can be chosen arbitrarily at any fixed temperature  $T$ . It directly enters into the definition of the infinite-temperature limit, as the effective 3-dimensional coupling constant  $g_3$  depends on  $g$  [20]. In the simplest case,  $g_3^2 \sim g^2(\mu)T$ . Comparing Eqs. (7-9) to those of the infinite-temperature limit [2], the constant of proportionality has to be 1 in this truncation scheme in order to obtain a smooth infinite-temperature limit. Hence, it only remains to choose the temperature dependence of  $\mu$ . As discussed in appendix A a t'Hooft-like scaling [21] with  $g^2 T$  fixed is employed to obtain a smooth infinite-temperature limit.

## 4 Infrared properties

Asymptotic freedom turns out to be advantageous for the infrared as well. Just at the phase transition, the  $n = 1$  Matsubara frequency has already an effective ‘mass’  $p_0 = 2\pi T_c \approx 1.7$  GeV. By the Appelquist-Carazzone theorem [22] the hard modes are suppressed by powers of  $|\mathbf{p}|/p_0$  in the infrared. Thus, hard modes do not contribute significantly. Therefore, the infrared behavior of the soft modes is the same as in the infinite-temperature limit and given by power-laws,

$$G(p) = A_g p^{-2\kappa}, \\ Z(p) = A_z p^{-2t}, \\ H(p) = A_h p^{-2l}.$$

The longitudinal function  $H$  behaves mass-like with  $l = 1$ . The exponents of the ghost and transverse gluon propagators are related as [2, 23]

$$\kappa = -\frac{1}{2} \left( t + \frac{1}{2} \right). \quad (10)$$

As in the infinite-temperature limit, always two solutions are found. One has  $\kappa = 1/2$  while the other has a weakly  $\zeta$ -dependent value, being  $\kappa = 0.39760$  at  $\zeta = 1$  [2, 23]. The latter is the more likely solution, at least in the infinite-temperature limit [2]. Hence the infrared exponents are independent of temperature and therefore at least gluons transverse w.r.t. the heat-bath are confined above the phase transition. Studying each equation in detail, it turns out that these quite general statements are implemented very differently in each equation.

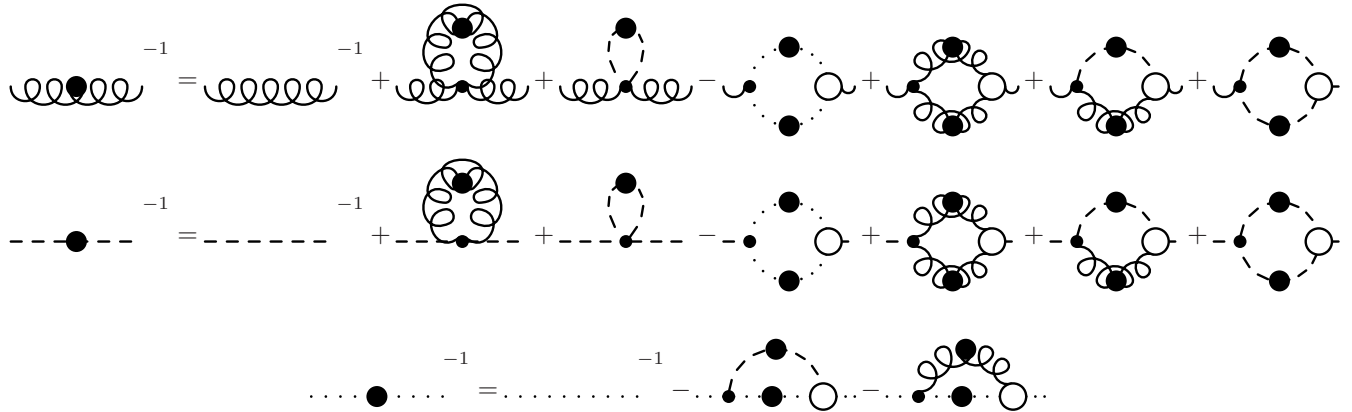


**Fig. 1.** The truncated Dyson-Schwinger equations at finite temperature. The dotted lines denote ghosts, the dashed lines longitudinal gluons and the wiggly lines transverse gluons. Lines with a full dot represent self-consistent propagators and small dots indicate bare vertices. The open circled vertices are full and must be constructed in a given truncation scheme. A bare ghost-gluon vertex and slightly modified bare gluon vertices have been used here. Note that for soft modes the ghost-longitudinal and the 3-point coupling of three longitudinal and of one longitudinal and two transverse gluons vanish.

In case of the hard modes, there is no purely soft contribution due to momentum conservation at the vertices. Thus they decouple and a self-consistent solution is that all hard-mode dressing functions are constant in the infrared.

In the case of the soft ghost equation (7), all contributions become constant in the infrared. Thus they can be canceled by the (renormalized) tree-level value. Only the subleading behavior remains, as in the case of the 3-dimensional and 4-dimensional theory [2,15]. As the subleading contribution of the purely soft term dominates the hard terms, the same behavior as in the infinite-temperature limit emerges.

In case of the transverse equation (9), the hard mode contributions give rise to mass-like  $1/p^2$  terms at best. These terms are subleading compared to the soft ghost-loop. Thus the infrared is dominated by the latter and the same infrared solution as in the infinite-temperature limit is found.

Finally, the longitudinal equation (8) is quite different from its equivalent in the 3-dimensional or 4-dimensional case. In the prior case, it was dominated by its tree-level mass, while in the latter it is identical to the transverse one. In the present case, the absence of pure soft interactions with ghosts, which could generate divergent contributions as in the transverse equation, leads to dominance of the hard modes<sup>3</sup>. These provide mass-like contributions in the infrared. Inspecting e.g.  $P$  at  $\xi = 1$

$$P(0, q_0, \mathbf{q}, \mathbf{p}) = \frac{|\mathbf{q}|^2 q_0^2 \sin \theta}{|\mathbf{p}|^2 q^2 (q_0^2 + (\mathbf{p} + \mathbf{q})^2)}, \quad (11)$$

and using the fact that the hard dressing functions are constant in the infrared, directly leads to a mass-like behavior due to the explicit  $1/|\mathbf{p}|^2$  factor and the finiteness

<sup>3</sup> The pure soft interactions represented by the kernels  $N_1$  and  $N_2$  only generate a constant term in the infrared. Without a tree-level mass, the soft tadpoles generate a contribution which can be removed by renormalization.

of the remaining expression. Thus, the 3-dimensional mass of the Higgs sector is generated dynamically by the interaction with the hard modes.

In conclusion, the infrared exponents of all soft mode dressing functions do not depend on the temperature. Only the infrared coefficients change.

These observations imply that, by using a finite number of Matsubara frequencies, it will not be possible to obtain the infrared 4-dimensional vacuum solutions. This would only be possible, if the infrared limit of the high-temperature and the low-temperature phase would have been both encoded in the soft interactions alone or, as the electric screening mass, would already be induced by a single hard mode. However, any finite number of modes will not be able to generate a divergence stronger than mass-like in the longitudinal equation, equivalent to the soft ghost contribution in the transverse equation. Hence, the 4-dimensional behavior can be established only by infinite summation. In this case, the generated mass has to diverge even after renormalization at  $p = 0$  to obtain the vacuum solution, providing over-screening instead of screening. The possibility that the ghost-gluon vertex changes due to temperature resulting in a coupling of soft ghost modes to soft longitudinal gluons at low temperature but not at high temperature is unlikely, since a bare ghost-gluon vertex is already sufficient at low temperatures and in the vacuum [6,15].

## 5 Truncation

Concerning the truncation chosen, all arguments proven to be successful in the vacuum and the infinite-temperature limit [2,15,19] also apply here. This includes the requirement that, due to the Gribov condition, the dressing functions  $G$ ,  $Z$ , and  $H$  have to be positive semi-definite. Hence the discussion here will only cover the additional aspects due to finite temperature. The main additional truncation

tion is to include only the finite set  $[-N + 1, N - 1]$  of Matsubara frequencies.

For large but still finite  $T$  the 3-dimensional limit is to be made explicit. Thus, all the problems encountered in the 3-dimensional theory [2] persist, including the necessity of a modified soft 3-gluon vertex. Hence, all modifications<sup>4</sup> of the pure soft terms will be left as in the case of [2], except for the tadpoles in the Higgs equation (8). Due to the dynamically generated mass, it will be necessary to alter this behavior. As no further information on the interaction vertices involving hard modes is available, the corresponding vertex functions will be assumed bare. Due to the large mass of the hard modes, such a tree-level ansatz should be justified.

The hard mode contributions induce additional spurious divergences. As they contribute to the two-point functions mostly at mid-momenta, when viewed from the 4-dimensional perspective using  $p^2 = p_0^2 + \mathbf{p}^2$ , it is expected that in the chosen truncation, they are much harder to compensate. This is indeed the case. The subtraction prescriptions are listed in appendix B. The technically quite involved construction is described in detail in ref. [19].

After removal of the spurious quadratic divergences, the resulting equations are still logarithmically divergent for  $N \rightarrow \infty$ . The integrals themselves are convergent, but the Matsubara sum is not, as the terms scale like  $1/q_0$ . Hence the sum diverges for an infinite number of Matsubara frequencies. This is the 4d logarithmic divergence and thus the usual one of Yang-Mills theory [25], which has to be renormalized appropriately. To this end, three regions of momentum are to be distinguished:

At  $p \leq 2\pi T$ , all terms in the Matsubara sums behave essentially the same due to the Appelquist-Carrazzone decoupling theorem. It is valid as the hard modes behave essentially tree-level-like. As the contributions of the hard modes behave as  $1/q_0$ , the final result will depend on the number of Matsubara frequencies included. Thus, it is necessary to renormalize in order to be independent of the cutoff, which is in this case imposed by the number of Matsubara frequencies included. The renormalization procedure will be implemented below. By this approach, the results can be made quite reliable in this regime.

At  $2\pi T \leq p \leq 2\pi T(N - 1)$ , more and more Matsubara terms depart from their  $1/q_0$  behavior to a  $1/p$  behavior. As the external momentum  $p$  becomes large compared to the effective mass  $q_0$  of a hard mode, the mode becomes dynamical and behaves like a massive 3-dimensional particle. The results are still quite reliable in this region, since also for  $N \rightarrow \infty$ , at any finite momentum  $p$  only a finite number of Matsubara frequencies are dynamical. It becomes less and less reliable when approaching the upper limit  $2\pi T(N - 1)$ .

<sup>4</sup> Recent investigations indicate that the three-gluon vertex may have an infrared divergence [24]. As pointed out also in ref. [24], this does not affect the infrared regime, as this range is dominated by the ghost loop. This is likely also the case at finite temperature in the transverse equation. Due to the chremoelectric screening it is conceivable that this behavior does not persist in the longitudinal equation at high temperatures.

At  $p \geq 2\pi T(N - 1)$ , the situation changes drastically. Opposite to the case  $N = \infty$ , all Matsubara modes are dynamical and their contributions will scale as  $1/p$ . Thus the number of Matsubara modes will now enter linearly instead of logarithmically. This is an artifact of cutting off the Matsubara sum. In this region the results are not reliable. However, as the sum is still finite and suppressed by  $1/p$ , the contribution is subleading with respect to the tree-level term and thus the system of equations can still be closed consistently<sup>5</sup>.

By renormalization, these artifacts can be reduced, if not completely removed at sufficiently small momenta. In that sense the finite Matsubara sum approximation is a small-(3-)momentum approximation. However, there are a few subtleties involved concerning the renormalization of a truncated Matsubara sum.

In the vacuum case [8, 17], the DSEs can be renormalized using a momentum subtraction scheme (MOM). This approach fails if the large momentum asymptotic value of the dressing functions is a constant different from 0. In the case of a truncated Matsubara sum, the ultraviolet behavior is that of a massive 3-dimensional theory. Thus the self-energy contributions vanish as  $1/p$  in the ultraviolet [2]. Therefore the dressing functions  $F = G, Z, H$  are dominated by the tree-level term

$$\lim_{|\mathbf{p}| \rightarrow \infty} F(p_0, |\mathbf{p}|) \rightarrow \frac{1}{Z_3}. \quad (12)$$

Here  $Z_3$  is generically the wave function renormalization of  $F$ . For a finite number of Matsubara frequencies  $Z_3$  is finite. Therefore the renormalization will here be performed by explicit counter-terms. This is discussed below.

A second point is the mass and mass renormalization necessary for the soft longitudinal mode. The soft mode with frequency  $p_0 = 0$  of the  $A_0$  component of the gauge field transforms homogeneously instead of inhomogeneously under gauge transformations. Therefore gauge symmetry permits to add a term

$$\delta m^2 A_0^2(0, \mathbf{p}) \quad (13)$$

to the Lagrangian. In the vacuum such a term is forbidden by manifest Lorentz invariance. At finite temperature in the Matsubara formalism, this is no longer the case, and such a term could in principle be present. This term replaces the  $p_0^2 A_0^2$  term of the hard modes, which stems from the  $A_0 \partial_0^2 A_0$  term in the Lagrangian for  $p_0 \neq 0$ .

Concerning the counter-terms, the wave-function renormalization is performed by adding the counter-term

$$\delta Z_3(A_\mu^a \partial_\mu \partial_\nu A_\nu^a - A_\mu^a \partial^2 A_\mu^a) \quad (14)$$

to the Lagrangian. In the case  $p_0 = 0$ , the first term is not present for the longitudinal mode  $A_0$ . Its place is taken by (13). This implies a relation between the wave-function counter-term  $\delta Z_3$  and the mass counter-term  $\delta m^2$ , which

<sup>5</sup> A further argument is that otherwise the corresponding finite 3-dimensional theory would be ill-defined which is not the case.

cannot be exploited here due to the truncation of the Matsubara sum. Therefore an independent renormalization of the wavefunction and the mass of the soft longitudinal mode is necessary and will be performed.

A last point concerns the implications for the counter-terms due to the truncation of the Matsubara sum. As the divergence structure must be the same as in the vacuum, the counter-terms must be the same for all frequencies. This is no longer the case when the Matsubara sum is truncated, as can be seen directly by counting. In the sum for the soft mode,  $p_0 = 0$ , contributions from  $2N - 1$  Matsubara modes are present for each loop. For the hard mode with  $p_0 = 2\pi T(N - 1)$ , only  $N$  contributions are present, as  $|p_0 + q_0| \leq 2\pi(N-1)T$ . Thus different numbers of modes contribute and the counter-terms cannot be the same. This is always the case as long as  $N < \infty$ . To surpass the problem in a constructive manner, each mode will be renormalized independently.

Therefore, a counter-term Lagrangian is added, given by

$$\begin{aligned} \delta\mathcal{L} = & \delta m^2 A_0^a(0)^2 + \sum_{q_0} \left( \delta Z_{3T}(q_0) A_\mu^a(q_0) \Delta_{T\mu\nu}(q_0) A_\nu^a(q_0) \right. \\ & + \delta Z_{3L}(q_0) A_\mu^a(q_0) \Delta_{L\mu\nu}(q_0) A_\nu^a(q_0) \\ & \left. + \delta \tilde{Z}_3(q_0) \bar{c}^a(q_0) \partial^2 c_a(q_0) \right) \end{aligned} \quad (15)$$

where  $A_\mu^a(q_0)$  are the modes of the gluon field and  $\bar{c}(q_0)$  and  $c(q_0)$  are the modes of the ghost and anti-ghost field, respectively.  $\Delta_{T/L\mu\nu}$  are the appropriate tensor structures of derivatives.

This shortcoming is a consequence of the truncation of the Matsubara sum, yielding incorrect ultraviolet properties: For large momenta the system under consideration is equivalent to a 3-dimensional theory of  $2N - 1$  particles per 4d particle species. In such a theory all fields can be renormalized independently. When the limit  $N \rightarrow \infty$  is performed, the wavefunction renormalizations will again coincide, as is shown<sup>6</sup> for  $\tilde{Z}_3$  in Fig. 2. However, this process is logarithmically slow.

In all equations, but the one for  $H(0, \mathbf{p})$ , using the counter-terms of (15) amounts to replacing the tree-level term 1 by  $1 + \delta Z_3 = Z_3$ . In this way multiplicative renormalization is obtained explicitly. In the equation for  $H(0, \mathbf{p})$ , the tree-level term is replaced<sup>7</sup> by  $1 + \delta Z_{3L} + \delta m^2/p^2$ . Thus, it also generates a mass-renormalization.

The last ingredient is the renormalization prescription, which will be taken as

$$F(s) = 1, \quad (16)$$

where  $s$  is the subtraction point. Here  $s = T$  is chosen, see [19] for an alternative. This also ensures  $G(s)^2 Z(s) = 1$  as is required in the 4-dimensional theory [15].

<sup>6</sup> For gluons, the value of the wavefunction renormalization, in the computationally accessible range of  $N$ -values, is dominated by  $N$ -dependent effects at mid-momenta. Hence, the logarithmic running is not easily discernible.

<sup>7</sup> Note that when using the projector (6), also  $\delta m^2$  is multiplied by  $\xi$ .

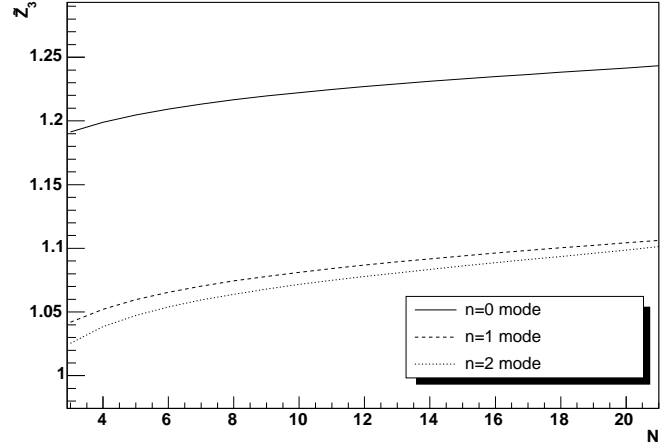


**Fig. 2.** Dependence of  $\tilde{Z}_3$  on the number of Matsubara frequencies  $N$  for the three lowest frequencies. Shown are the values for the  $g = 1/2$  solution at  $T = 1.5$  GeV. The solution for  $g \approx 0.4$  is very similar, even on a quantitative level.

In case of  $H(0, \mathbf{p}^2)$ , two prescriptions are necessary. The first is<sup>8</sup>

$$\lim_{|\mathbf{p}| \rightarrow 0} |\mathbf{p}|^{-2} H(0, \mathbf{p}^2) = \frac{1}{m_{3d}^2} = \frac{1}{r^2 g^4 T^2 + g^2 T C_A \frac{r g^2 T}{4\pi}} \quad (17)$$

where  $m_{3d}$  is the tadpole-improved mass of the 3-dimensional theory [2]. It depends on  $r = m_h/g_3^2$ , which is again taken to be the same value as in ref. [2]. For fixed  $g_3$ , this mass is independent of temperature. In addition,

$$\frac{1}{H(0, s)} = 1 + \frac{m_{3d}}{s^2} \quad (18)$$

is required to fix the wavefunction renormalization.

It should be noted that, by renormalizing at  $T$ , it is guaranteed that the correct 3-dimensional limit is obtained. This prescription requires that at  $T \rightarrow \infty$  all dressing functions approach 1 at infinity [2].

Therefore, the explicit implementation of the renormalization prescription for the DSE of a dressing function  $F$  with self-energy contributions  $I$

$$\frac{1}{F(p)} = 1 + I(p) \quad (19)$$

is then

$$\begin{aligned} \frac{1}{F(p)} &= 1 + \delta Z_3 + I(p) \\ \delta Z_3 &= -I(s) \end{aligned}$$

and in the case of  $H(0, \mathbf{p}^2)$

$$\frac{1}{H(0, \mathbf{p}^2)} = 1 + \delta Z_{3L} + \frac{\delta m^2}{p^2} + I(p)$$

<sup>8</sup> For numerical reasons, it is actually performed at  $2\delta_i$ , where  $\delta_i$  is the numerical IR-cutoff of the integration. This causes only a marginal difference.

$$\delta m^2 = m_r^2 - \lim_{p \rightarrow 0} p^2 I(p)$$

$$\delta Z_{3L} = -I(s) + \frac{\lim_{p \rightarrow 0} p^2 I(p)}{s^2},$$

where  $m_r = m_{3d}$  is the renormalized mass.

## 6 Numerical results

### 6.1 Propagators

Here the full system of Eqs. (7-9) at all momenta will be treated<sup>9</sup>. The numerical method employed is discussed in ref. [19,26].

For  $N = 12$  independent Matsubara frequencies, the result is shown in Fig. 3 for both sets of infrared exponents,  $\kappa = 1/2$  and  $\kappa = 0.39760$ . There are several observations. First of all, in the infrared the soft modes are nearly unaffected by the presence of the hard modes. The latter show a significant modification, compared to tree-level, although still only of the order of 30%. The plateau reached in the ultraviolet is an artifact of the truncation, yielding a finite wave-function renormalization. The hard-mode dressing functions exhibit some structure. There are maxima in all dressing functions at mid-momenta. This is most pronounced in the case of the dressing functions of the longitudinal gluon. These structures do not translate into a corresponding structure in the propagators, which are monotonically decreasing from a constant of order  $1/p_0^2$  in the infrared to 0 in the ultraviolet. For the hard-mode dressing functions it is also nearly irrelevant to which of the two soft infrared solution they belong.

In general, the hard modes deviate less from unity with increasing  $n$ . The only exception seems to be the ultraviolet behavior of the  $n = 1$  gluon modes. This is, however, an artifact of the truncation. If the Matsubara sum would not be truncated, all dressing functions would go to zero for sufficiently large momenta. On the other hand, the finite value attained due to the truncation can be influenced by the requirement to fit continuously to the mid-momentum behavior. Hence, due to the peaks at mid-momenta in the gluon dressing functions, the ultraviolet plateau is increased for the  $n = 1$  dressing functions, leading to the level reordering. If the peaks would be larger, this would also affect further modes. In the limit of  $N \rightarrow \infty$ , the peaks reach a finite maximum and therefore permit the plateaus all going to zero, thus restoring the correct behavior.

Fig. 4 displays the dependence of the full solutions on the number of Matsubara frequencies. While the soft-mode dressing functions are nearly unaffected, apart from

<sup>9</sup> A separate discussion of a further truncation, the ghost-loop only truncation, can be found in ref. [19]. This truncation includes only tree-level and loop diagrams with at least one ghost-line. These results support that it is indeed the ghost sector which drives the infrared behavior of Yang-Mills theory, also at finite temperature, in accordance with the Gribov-Zwanziger scenario.

the value of the renormalization constants, the effect on the hard mode dressing functions is significant. The ghost is quite insensitive, except for its wave-function renormalization. This is not the case for the gluons. The peaks at mid-momentum are sensitive to the number of Matsubara frequencies included. The effect is largest for the longitudinal gluon dressing functions. From the available number of Matsubara frequencies, it is hard to estimate whether the peak grows to a finite value for an infinite number of Matsubara frequencies or not. It therefore cannot be excluded that the hard longitudinal gluon dressing functions violate the Gribov condition, once sufficiently many Matsubara frequencies are included. This would be very similar to the case of the transverse gluon dressing function in the infinite-temperature limit [2] and therefore would necessitate a similar vertex construction for the longitudinal-gluon-transverse-gluon vertex as for the soft transverse gluon vertex. If such a vertex would be necessary, the result would be a finite peak, very similar to the present situation. Thus, the results would be even quantitatively quite similar.

The disappearance of the peaks in the gluon dressing functions at  $N = 2$  can be directly related to the vanishing of hard-mode couplings due to the restriction  $(p_0 + q_0)/(2\pi T) < 2$ . Only hard-soft-mode couplings contribute. Thus, the peak is generated solely due to pure hard-hard interactions.

In general, the  $n > 1$  modes essentially follow the behavior of the  $n = 1$  mode, albeit much closer at tree-level.

The dependence on temperature is shown in Fig. 5. The infrared coefficients for the soft modes of the ghost and transverse gluon dressing functions are affected, while the dressing function of the longitudinal gluon only changes slightly at mid-momenta. Therefore, the dressing function of the longitudinal gluon is dominated by its renormalized mass also when changing the temperature. As expected, the hard-mode dressing functions become more and more tree-level like with increasing temperature. The peaks in the hard mode dressing functions shift to higher momenta, owing to the renormalization condition, and become smaller due to the increase of the effective mass  $p_0$  of the hard modes. At infinite temperature, they smoothly merge into the corresponding 3-dimensional solutions. At low temperatures, the opposite effect is observed. In general, the hard-mode dressing functions become more dynamical as their effective mass decreases, albeit quite slowly. The insensitivity on the infrared solution of the soft sector is not changed when reducing the temperature, and it may need a significantly lower temperature to induce a change.

Employing t'Hooft scaling, the lowest temperatures that can be achieved with a numerically stable solution are of the order of 750 MeV. Using a temperature-independent renormalization scale and subtraction point [19] instead results merely in a shift in the onset of nonperturbative effects to larger momenta with some deformations, necessary to obey the renormalization conditions. In this case, it was also possible to cool down to  $T = 140$  MeV, indicating the possibility of super-cooling.

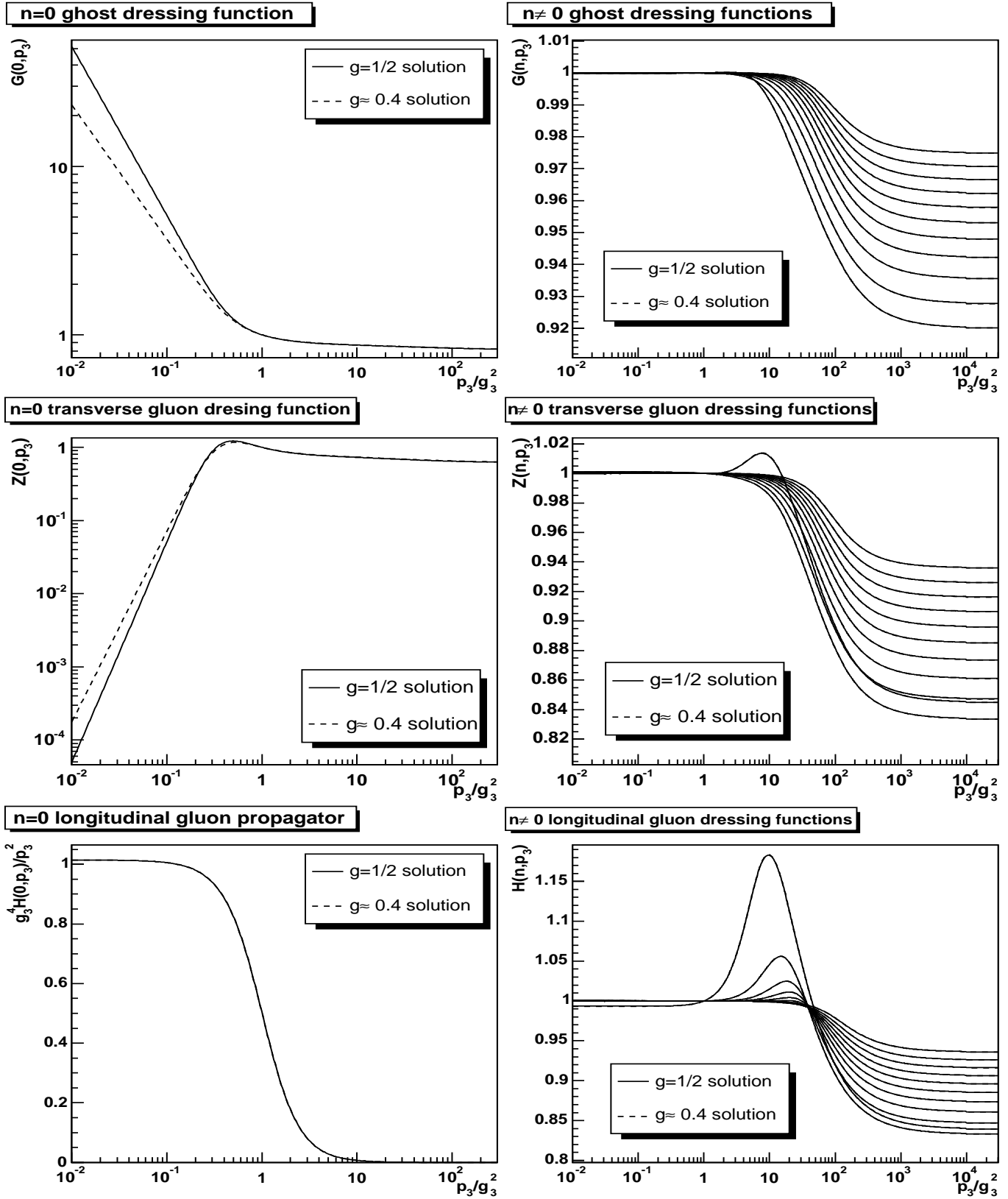


**Fig. 3.** From top to bottom, the left panels show the dressing functions for the soft modes of the ghost and transverse gluon and the propagator of the longitudinal gluon. The right panels display the hard-mode dressing functions  $n = 1$  to  $n = 11$ . Higher  $n$  correspond to lesser deviation from unity except for  $n = 1$ , see text. The solid lines are the  $g = 1/2$  solution and the dashed lines the  $g \approx 0.4$  solution. Both are taken at  $T = 1.5$  GeV,  $\zeta = \xi = 1$ , and  $N = 12$ . Note the different momentum scale in the left and the right panels.

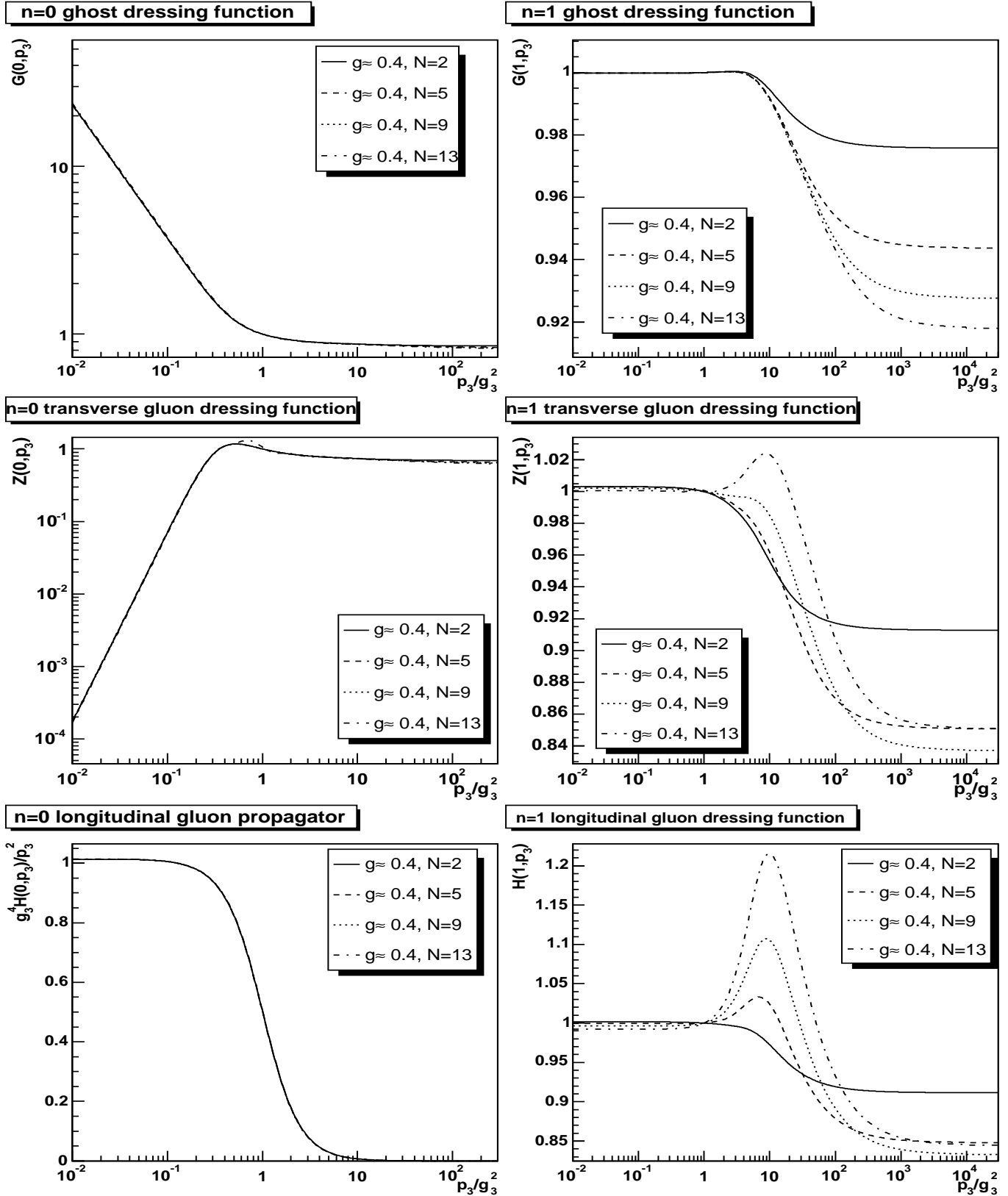


**Fig. 4.** The dependence of the solutions on  $N$  at  $T = 1.5$  GeV and  $\zeta = \xi = 1$ . For the soft modes from top to bottom the left panels show the dressing functions of the ghost and transverse gluon and the propagator of the longitudinal gluon. The right panels give the dressing functions for the  $n = 1$  hard mode. Only the  $g \approx 0.4$  solution is shown. The  $g = 1/2$  solution is similar and can be found in ref. [19]. The solid lines denote  $N = 2$ , dashed are  $N = 5$ , dotted  $N = 9$  and dashed-dotted  $N = 13$ .

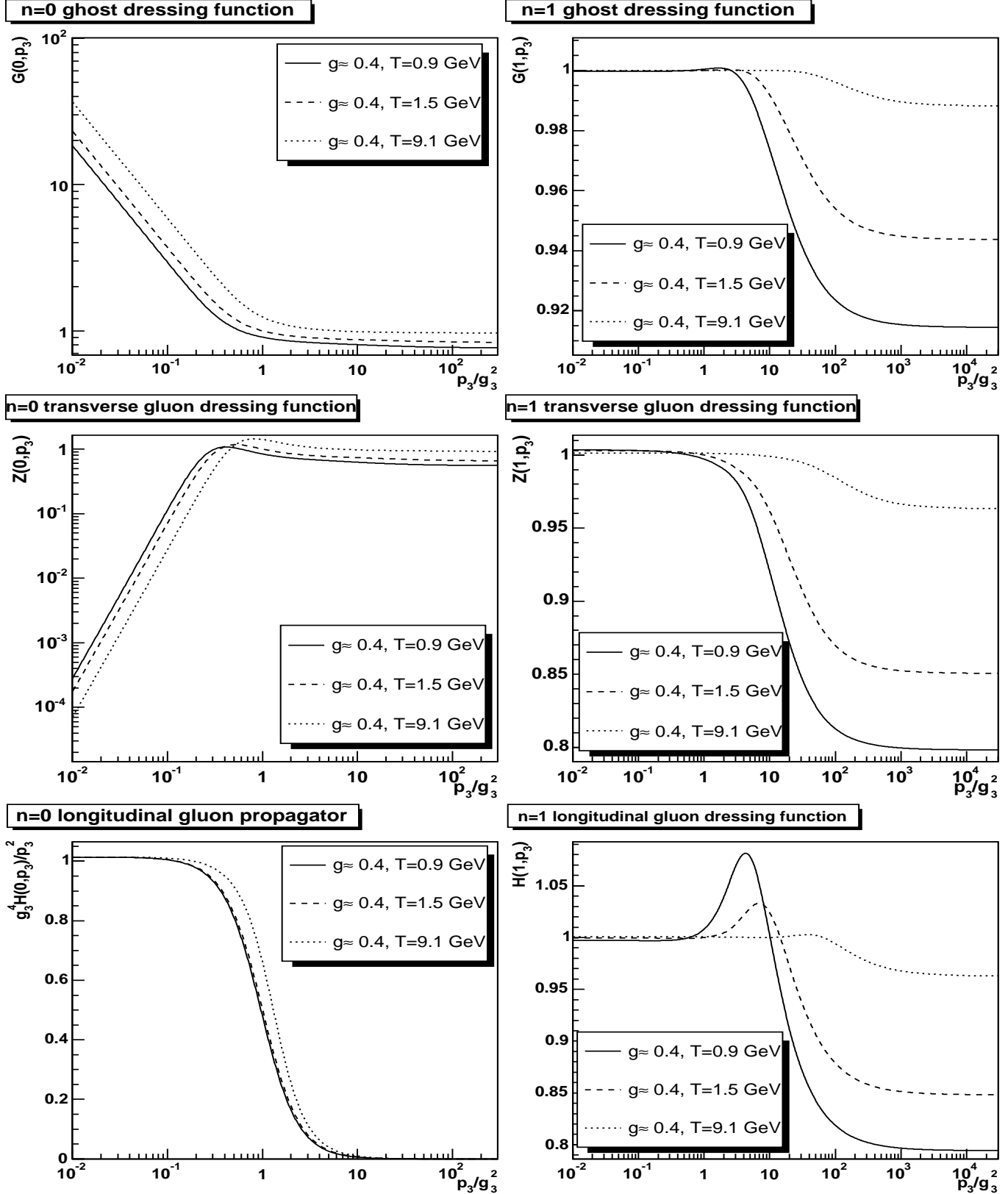


**Fig. 5.** The dependence of the solutions on  $T$  at  $N = 5$  and  $\zeta = \xi = 1$ . The left panel shows the soft modes, where apart from the longitudinal gluon the dressing functions are shown. In the latter case the propagator is shown. The right panels show the dressing functions for the  $n = 1$  hard mode. Only the  $g \approx 0.4$  solution is shown, the  $g = 1/2$  solution is similar and can be found in ref. [19]. Solid lines denote  $T = 0.9$  GeV, dashed lines  $T = 1.5$  GeV, and dotted lines  $T = 9.1$  GeV.

Varying the projection parameter  $\zeta$  leads to similar variations for the soft-mode dressing functions as in the 3-dimensional case [2]. The largest effect is seen in the infrared. As the hard-mode dressing functions are insensitive to the infrared behavior of the soft modes due to their effective mass, there are only weak variations of them with  $\zeta$ . Only at small  $\zeta$  an additional structure appears in the transverse gluon dressing function. This is likely due to the cross-term in Eq. (9). The effect of varying  $\zeta$  on the longitudinal sector is negligible, as in the 3-dimensional case. Correspondingly, the effect of varying  $\xi$  is only significant for the longitudinal sector. The sensitivity is much less pronounced then in the case of varying  $\zeta$ . Especially, the soft longitudinal dressing function is nearly unaffected by variation of  $\xi$ . The reason is that the soft equation does not depend explicitly on  $\xi$ , as it can be divided out of the equation for  $\xi \neq 0$ . Therefore, any  $\xi$  dependence enters only indirectly by the weak dependence of the hard modes on  $\xi$ . Only in the case of  $\xi \approx 0$  significant effects are found, owing to the pathology of the  $\xi = 0$  case. Details of the dependence on  $\zeta$  and  $\xi$  can be found in ref. [19]. The dependence on the three-gluon vertex construction is qualitatively not different from the infinite-temperature limit for the soft modes, and negligible for the hard modes [19].

At this point, a comparison to a different approach to obtain the high-temperature gauge propagators can be made. The usual continuum method is the semi-perturbative hard thermal loop (HTL) approach [27]. It is based on resumming the hard mode contributions in self-energy diagrams. In the transverse infrared sector it is plagued by severe problems, due to its perturbative nature. The final result is a transverse gluon propagator with a particle-like pole at  $p = 0$ . Thus the gluon exponent  $t$  would vanish. This is in sharp contrast to the results found here and, as discussed in ref. [2], such an infrared behavior is not very likely. Also the lattice results in the infinite-temperature limit [28] and at temperatures somewhat above the critical [29] support the results found here. On the other hand, concerning the soft longitudinal mode and the hard modes, HTLs and the ansatz presented here find qualitatively similar results on the level of the propagators.

## 6.2 Thermodynamic potential

Concerning the contribution from the hard modes to the thermodynamic potential, it is problematic to use the approach of Luttinger-Ward / Cornwall-Jackiw-Tomboulis (LW/CJT) [30], as done previously [2,6]. In the present truncation scheme the 2PI contribution in the LW/CJT-action are neglected, and thus only the interaction part is considered. This latter part vanishes identically for a free system, i.e. for a system containing only tree-level dressing functions. This free contribution has thus to be added explicitly. Therefore, the hard-mode contribution, being essentially tree-level, can be calculated up to perturbative corrections to be the same as that of a non-interacting system of free gluons. The LW/CJT-expression does not

capture the tree-level contribution of the soft modes, and it thus can be added here. This yields a thermodynamic potential of a gas of massless gluons with small corrections due to the explicit soft-mode contributions and the residual interactions of the hard modes. For  $N_c = 3$  it is given by [1]

$$\lim_{T \rightarrow \infty} \frac{\Omega}{T^4} = -\frac{16\pi^2}{90}. \quad (20)$$

Using t'Hooft-scaling for the interaction strength, the corrections due to the soft contributions obtained by the LW/CJT action vanish most likely as  $1/T$  [2,19]. The only remaining contribution in the infinite-temperature limit is hence the Stefan-Boltzmann-contribution (20), in agreement with results from lattice calculations [1]. Therefore, the thermodynamic properties of the high-temperature limit are governed by the hard modes. However, as the calculation of the thermodynamic potential is problematic in the current approach [2,19], this can only be taken as an indication for such a behavior.

At temperatures of the order of the phase transition, the contribution of the soft modes to the thermodynamic potential is probably non-negligible. Furthermore, as discussed in ref. [31], these contributions can be highly relevant to the pressure  $p$  and lead to a non-vanishing value for the trace of the stress-energy tensor,  $\epsilon - 3p$ , where  $\epsilon$  is the energy density. The vanishing of the trace would be expected for an ideal gas. Such an effect cannot be provided by perturbation theory [31], but has been observed in lattice calculations [1].

## 6.3 Schwinger functions

As stated in section 2, an unambiguous sufficient (although not necessary) signal for the confinement of a particle is a violation of positivity. This can be investigated using the Schwinger function, defined as

$$\Delta(t) = \frac{1}{\pi} \int_0^\infty dp_0 \cos(tp_0) \frac{F(p_0)}{p_0^2}, \quad (21)$$

where  $F$  is either  $Z$  or  $H$ . In the infinite-temperature limit a clear signal for positivity violation has been found for the transverse gluon [2]. However, for the longitudinal gluon no unambiguous signal could be found. It is therefore interesting to repeat the study at lower temperatures. The results are shown in Fig. 6.

The hard modes do not show a clear sign of oscillation within the available precision. Compared to the high-temperature case, a much clearer signal for positivity violation is found in the longitudinal propagator. Furthermore, the longitudinal Schwinger function is much more similar to the transverse one. Therefore, the contribution from the hard modes seem to be negative, shadowing the oscillations induced by the soft modes in the infinite-temperature limit. It is also this observation, which restricts the reliability of the result. Nonetheless, these results substantiate the non-triviality also of the longitudinal sector and requires further attention.

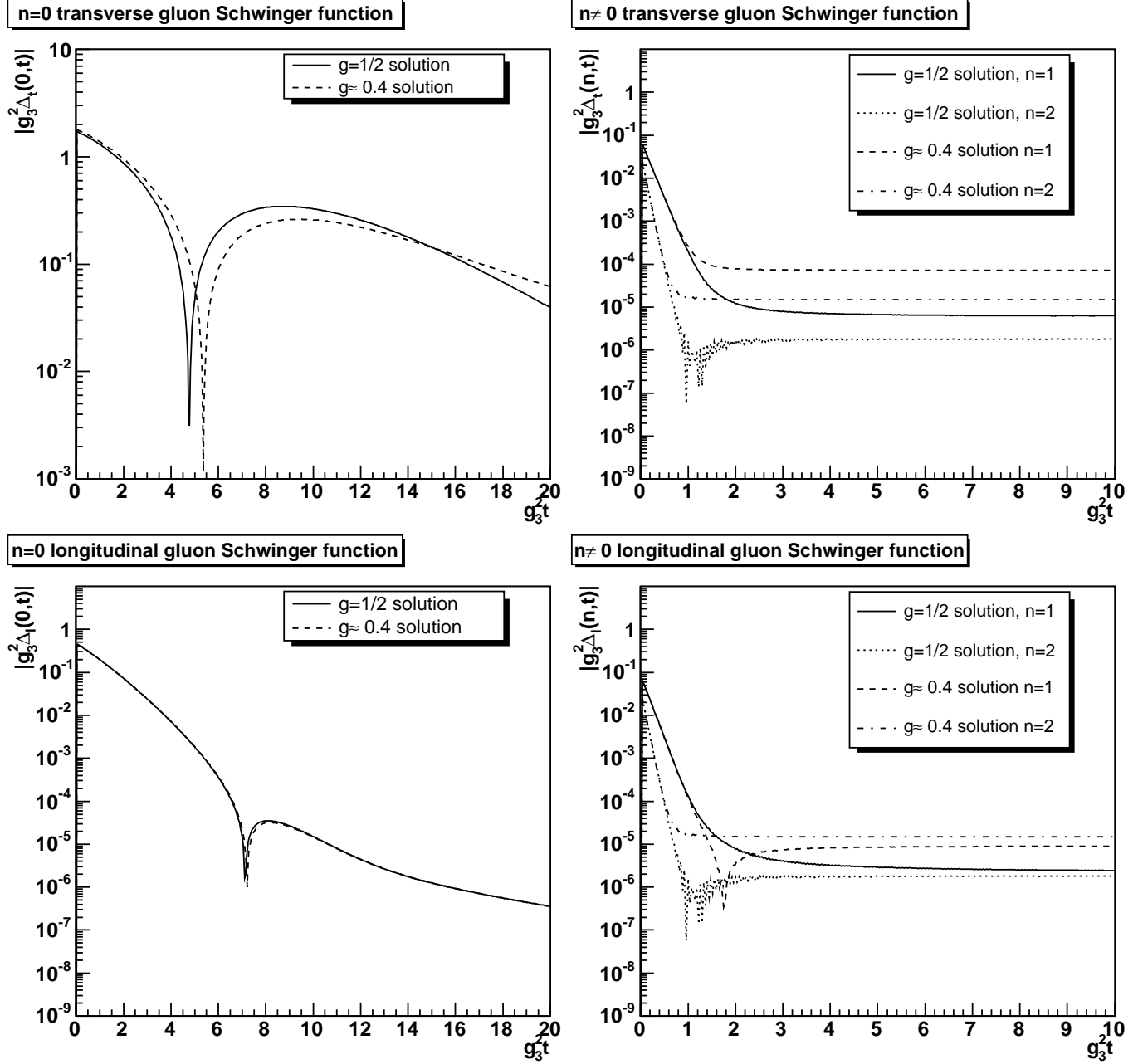


**Fig. 6.** The Schwinger function for the gluon propagator. The left panels show the results for the soft modes and the right panels for the hard modes with  $n = 1$  and  $n = 2$ . The top panels give the results for the transverse propagator and the bottom panels for the longitudinal propagator. The temperature is  $T = 1.5$  GeV,  $\zeta = \xi = 1$ , and  $N = 5$ . The result has been obtained with roughly half a million Fourier frequencies [19].

## 7 Discussion

Before discussing further the implications of the results found here on the structure of the Yang-Mills phase diagram, it is worthwhile to take a step back to gather and assess the findings. Especially, the reliability of the results deserves special attention.

The reliability of the exploratory study of finite temperature effects presented here and thus of the properties of the hard modes is a major concern. The success

of the truncation scheme in the infinite-temperature limit is based on its exactness in the ultraviolet and its presumed exactness in the infrared. Thus the consequences of the deficiencies at intermediate momenta are strongly constrained. This constraint is lost by cutting off the Matsubara sums. As a consequence, the ultraviolet properties of the hard modes are incorrect and a rooting in perturbation theory is prevented. This amplifies the second problem. The hard modes do not reach into the 4-dimensional infrared region due to their effective mass. Therefore the

advantages of the truncation scheme are lost to a large extent and the equations for the hard modes become unreliable.

Nonetheless, the presented results are relevant. At sufficiently large temperatures, the truncation-dependent self-energies of the hard modes are suppressed by the large effective mass and they are dominated by the truncation-independent tree-level terms. Thus, the truncation artifacts vanish when the temperature goes to infinity. The difficult part is then to assess down to which temperature the results are still reliable, at least qualitatively.

As it is found that the system is only very weakly dependent on temperature, qualitative conclusions can probably be drawn even at quite small temperatures. This is due to the fact that the infrared properties of the soft modes are nearly independent of the hard modes. In general, the hard modes effectively decouple because of their effective mass, which is large compared to  $\Lambda_{QCD}$ , even at the phase transition. The only exception is the generation of the screening mass for the soft longitudinal gluon, which can be found on quite general grounds and thus can be considered reliable. This is also supported by the systematic error estimations performed in refs.[2, 19], which do not find qualitative effects but only small quantitative ones.

Although the quantitative results may be subject to change, the qualitative result is expected to be quite reliable. Probably down to temperatures within the same order of magnitude as the phase transition, the high-temperature phase consists of strongly interacting soft modes exhibiting confining properties and inert hard modes. This is supported by lattice results, which find that the infinite-temperature limit is effectively reached at about  $2T_c$  [28] and the qualitative features of the infinite-temperature limit up to the highest temperatures, for which propagators are available, of  $6T_c$  [29]. This constitutes the major result found in this work.

Concerning the thermodynamic potential, no final conclusion can be drawn. The results indicate that the gross thermodynamic properties far away from the phase transition are completely dominated by the hard modes and that a Stefan-Boltzmann behavior is reached in the infinite-temperature limit. Considering the crude assumptions made and the difficulties encountered, this result is indicative at best. Nonetheless, if it can be substantiated, this would allow to understand how a Stefan-Boltzmann-like behavior can emerge from a non-trivial theory. At the same time, the results also indicate that, at low temperatures, nonperturbative effects will play a role in the thermodynamics and certainly will especially be relevant in the vicinity of the phase transition.

## 8 Concluding remarks

Looking at the results found in ref. [2, 19] and the solutions at zero [15] and small temperatures [6], a coherent picture emerges. Still, this picture is overshadowed by the problems of truncation artifacts, especially at finite temperatures.

The main difference between the low-temperature and the high-temperature phase is not primarily one between a strongly interacting and confining system and one with only quasi-free particles. The chromoelectric gluons, whose infrared behavior change from over-screening to screening, come somewhat close to such a picture, and the hard modes certainly do. The latter become free due to the vacuum property of asymptotic freedom and the dependence of their energy on the temperature, thus in an expected although not entirely trivial manner. The chromomagnetic gluons remain over-screened in the infrared and are thus confined. In the sector transverse to the heat-bath, the results provide strong evidence for the Zwanziger-Gribov and/or the Kugo-Ojima scenarios, even at very high temperatures.

Including the observation of super-heating in the low-temperature regime [6] and super-cooling at high temperatures, the scenario emerging is a chromoelectric phase transition of first order. This phase transition connects two different strongly interacting phases of Yang-Mills theory. Especially quantum fluctuations always dominate thermal fluctuations and at least part of the gluon spectrum is always confined.

In the vicinity of the phase transition, the consequences of nonperturbative effects are likely also relevant to thermodynamic properties, especially to the pressure and the trace anomaly [31]. This underlines the importance of non-perturbative effects at least for the temperature range relevant to experiment.

In summary, evidence is found that, in the high-temperature phase of Yang-Mills theory, the elementary excitations exhibit quite non-trivial correlations. The soft interactions are non-trivial at all temperatures, and the decoupling of the hard modes is evident. This establishes the main features of the high-temperature phase of Yang-Mills theories in Landau gauge. The results found here comply with Gribov-Zwanziger or Kugo-Ojima type confinement mechanisms for the dimensionally reduced theory. Therefore, the high-temperature phase is definitely non-perturbative. It will be interesting to investigate the consequences for quarks and their correlations at high temperature on the one hand and for cosmology and the early universe on the other.

The authors are grateful to Burghard Grüter for valuable discussions and to Jan M. Pawłowski for a critical reading of the manuscript and helpful remarks. This work was supported by the BMBF under grant numbers 06DA116 and by the Helmholtz association (Virtual Theory Institute VH-VI-041).

## A Running coupling

For fixing the coupling there are two options to consider.

If  $\mu$  is fixed,  $g_3 = g^2 T$  grows without limit as  $T$  grows. This does not necessarily pose a problem, as the infinite-temperature propagators are independent of  $g_3$  as long as they are expressed as a function of  $p/g_3^2$  [2]. Under such circumstances, all momenta below  $T$  are effectively infrared, and the nonperturba-

tive regime would extend to all momenta. Here this possibility will not be pursued any further<sup>10</sup>.

Alternatively, it is possible to use the limiting prescription  $g^2(\mu(T))T = c_\infty$ , where  $c_\infty$  is an arbitrary constant, effectively performing a renormalization group transformation when changing the temperature. This fixes  $g_3^2$  to be proportional to  $\Lambda_{QCD}$ , the dynamical scale of QCD [25], while the 4-dimensional coupling vanishes like  $1/T$ . This defines a t'Hooft-like scaling in  $T$ . Note that  $g \rightarrow 0$  for  $T \rightarrow \infty$  corresponds to the conventional arguments of a vanishing coupling in the high-temperature phase [27]. However, as in the large- $N_c$  limit, a t'Hooft-scaling is performed, generating a well-defined theory. Hence, this possibility defines a smooth 3-dimensional limit with a finite 3-dimensional coupling constant. Here  $c_\infty = 1$  is chosen.

Furthermore, it would be useful to give explicit units for the temperature scale. In the vacuum, the scale is fixed via a comparison of the running coupling to perturbation theory [17]. This is not possible here because the Matsubara sum is truncated, and the coupling cannot be calculated reliably for momenta of the order of  $2\pi NT$ .

The simplest procedure is to compare  $g_3$  to lattice calculations. There, the effective 3-dimensional coupling is found to be  $g_3^2(2T_c)/2T_c = 2.83$  [28]. The phase transition temperature is  $T_c = 269 \pm 1$  MeV [1]. Albeit this will not be exactly  $g^2 \cdot 2T_c$  due to the truncation, a first approximation is to require the same temperature scale at  $2T_c$ . Using the fixed  $g^2 T = c_\infty$  prescription, then  $1 = c_\infty/(2T_c \cdot 2.83)$ . Since here  $c_\infty = 1$  in internal units, internal units have to be multiplied by 1.5 GeV to yield physical units. This temperature scale is used in section 6. The ratios of temperatures are independent of this prescription.

## B Subtraction of spurious divergences

The spurious divergences in contributions of hard modes due to the integration are dealt with in exactly the same way as in 3 dimensions [2] by adjusting the tadpole terms. Each integration kernel  $K$  in the longitudinal equation is split as

$$K = K_0 + K_D \quad (22)$$

where  $K_0$  is finite and  $K_D$  divergent upon integration. Each kernel  $K_D$  will be compensated by the corresponding tadpole in (8).

A new kind of spurious divergences appear when performing the Matsubara sum. When including more and more Matsubara frequencies, it is found that their contribution in the gluon equations (8) and (9) at  $|\mathbf{p}| < \max(q_0)$  scales as  $q_0$ , thus behaving as a quadratic divergence. This is an artifact of using a finite number of Matsubara frequencies and does not vanish as long as the number of frequencies is finite, no matter how large the number. This behavior is spurious and must be removed.

This can be performed by the replacement

$$F(q, q_0)F(p + q, q_0 + p_0) \rightarrow \left( F(q, q_0) - \frac{1}{Z_3} \right) \left( F(q + p, q_0 + p_0) - \frac{1}{Z_3} \right), \quad (23)$$

in all affected loops in the gluon equations.  $F$  is a generic dressing function and  $Z_3$  its wave-function renormalization.

<sup>10</sup> See [19] for a thorough discussion of this case

In the transverse equations all spurious divergences, including the one of the Matsubara sum, are again removed at  $\zeta = 3$ . Therefore, the replacement (23) will only be necessary in those contributions which are proportional to  $(\zeta - 3)$ . Hence the integral kernels are split differently than in (22) as

$$K(\zeta) = K_0 + (\zeta - 3)K_3 + K_D(\zeta). \quad (24)$$

Here  $K_0$  and  $K_3$  are finite and independent of  $\zeta$ , and  $K_D$  contains all divergences upon integration. The corresponding subtraction is then performed by the replacement

$$KF(q)F(p + q) \rightarrow K_0F(q)F(p + q) + (\zeta - 3)K_3 \left( F(q) - \frac{1}{Z_3} \right) \left( F(p + q) - \frac{1}{Z_3} \right). \quad (25)$$

In the soft transverse equation it is necessary in addition to remove tadpole-like structures at  $\zeta \neq 3$  in  $K_3$  [19], which alters (25) to

$$KF(q)F(p + q) \rightarrow K_0F(q)F(p + q) + (\zeta - 3) \left( K_3 - \frac{1}{p^2} \left( \lim_{p \rightarrow 0} p^2 K_3 \right) \right) \cdot \left( F(q) - \frac{1}{Z_3} \right) \left( F(p + q) - \frac{1}{Z_3} \right).$$

## References

1. F. Karsch and E. Laermann, arXiv:hep-lat/0305025 and references therein; D. H. Rischke, Prog. Part. Nucl. Phys. **52** (2004) 197 [arXiv:nucl-th/0305030] and references therein; F. Karsch, Lect. Notes Phys. **583** (2002) 209 [arXiv:hep-lat/0106019] and references therein.
2. A. Maas, J. Wambach, B. Grüter and R. Alkofer, Eur. Phys. J. **C37**, No.3, (2004) 335 [arXiv:hep-ph/0408074].
3. T. Kugo and I. Ojima, Prog. Theor. Phys. Suppl. **66** (1979) 1.
4. V. N. Gribov, Nucl. Phys. B **139** (1978) 1;
5. D. Zwanziger, Phys. Rev. D **69** (2004) 016002 [arXiv:hep-ph/0303028] and references therein.
6. B. Grüter, R. Alkofer, A. Maas and J. Wambach, arXiv:hep-ph/0408282.
7. F. J. Dyson, Phys. Rev. **75** (1949) 1736, J. S. Schwinger, Proc. Nat. Acad. Sci. **37** (1951) 452, Proc. Nat. Acad. Sci. **37** (1951) 455.
8. R. Alkofer and L. von Smekal, Phys. Rept. **353**, 281 (2001) [arXiv:hep-ph/0007355]; C. D. Roberts and S. M. Schmidt, Prog. Part. Nucl. Phys. **45** (2000) S1 [arXiv:nucl-th/0005064].
9. J. I. Kapusta, “Finite Temperature Field Theory” (Cambridge University Press, Cambridge, 1989).
10. W. Schleifenbaum, A. Maas, J. Wambach and R. Alkofer, arXiv:hep-ph/0411060 and references therein.
11. R. Oehme and W. Zimmermann, Phys. Rev. D **21** (1980) 1661. R. Oehme and W. Zimmermann, Phys. Rev. D **21** (1980) 471.
12. T. Kugo, arXiv:hep-th/9511033.
13. A. Cucchieri, T. Mendes and A. Mihara, JHEP **0412** (2004) 012 [arXiv:hep-lat/0408034]; A. Mihara, A. Cucchieri and T. Mendes, arXiv:hep-lat/0408021.
14. W. Schleifenbaum, A. Maas, J. Wambach and R. Alkofer, arXiv:hep-ph/0411052.

15. L. von Smekal, A. Hauck and R. Alkofer, *Annals Phys.* **267** (1998) 1 [arXiv:hep-ph/9707327]; L. von Smekal, R. Alkofer and A. Hauck, *Phys. Rev. Lett.* **79** (1997) 3591 [arXiv:hep-ph/9705242].
16. J. C. Taylor, *Nucl. Phys. B* **33** (1971) 436.
17. C. S. Fischer and R. Alkofer, *Phys. Lett.* **B536**, 177 (2002) [arXiv:hep-ph/0202202]; C. S. Fischer, R. Alkofer and H. Reinhardt, *Phys. Rev. D* **65** (2002) 094008 [arXiv:hep-ph/0202195].
18. C. S. Fischer, PhD thesis, U. of Tübingen, arXiv:hep-ph/0304233.
19. A. Maas, PhD thesis, Darmstadt U. of Technology, arXiv:hep-ph/0501150.
20. K. Kajantie, M. Laine, K. Rummukainen and M. E. Shaposhnikov, *Nucl. Phys. B* **458** (1996) 90.
21. G. 't Hooft, *Nucl. Phys. B* **72** (1974) 461.
22. T. Appelquist and J. Carazzone, *Phys. Rev. D* **11** (1975) 2856.
23. D. Zwanziger, *Phys. Rev. D* **65** (2002) 094039 [arXiv:hep-th/0109224].
24. R. Alkofer, C. S. Fischer and F. J. Llanes-Estrada, *Phys. Lett.* **B611** (2005) 279 [arXiv:hep-th/0412330].
25. M. Bohm, A. Denner and H. Joos, "Gauge Theories Of The Strong And Electroweak Interaction," Stuttgart, Germany: Teubner (2001) 784 p.
26. A. Maas, to be published.
27. J. P. Blaizot and E. Iancu, *Phys. Rept.* **359** (2002) 355 [arXiv:hep-ph/0101103] and references therein.
28. A. Cucchieri, F. Karsch and P. Petreczky, *Phys. Rev. D* **64** (2001) 036001 [arXiv:hep-lat/0103009].
29. A. Nakamura, T. Saito and S. Sakai, *Phys. Rev. D* **69** (2004) 014506 [arXiv:hep-lat/0311024].
30. J. M. Luttinger and J. C. Ward, *Phys. Rev.* **118** (1960) 1417; J. M. Cornwall, R. Jackiw and E. Tomboulis, *Phys. Rev. D* **10** (1974) 2428.
31. D. Zwanziger, arXiv:hep-ph/0407103.